Residual-stress Measurement Using Surface Displacements Around an Indentation

An experimental method for measuring the direction and magnitude of residual stress in metals by using optical interference to analyze the nonsymmetrical surface deformation around a shallow spherical indentation

by John H. Underwood

ABSTRACT—An experimental method is described which can measure the direction and magnitude of residual and applied stress in metals. The method uses optical interference to measure the permanent surface deformation around a shallow spherical indentation in a polished area on the metal specimen. The deviation from circularly symmetrical surface deformations is measured at known values of applied stress in calibration specimens. This deviation from symmetry can then be used to determine the direction and magnitude of tensile residual stress in specimens of the same material. Determination of compressive residual stress is more limited.

A model of the indentation process is offered which qualitatively describes experimental results in 4340 steel for both tensile and compressive stress. The model assumes that the deformation around an indentation is controlled by stresses analogous to those around a hole in an elastic plate. Various conditions are discussed which affect the indentation process and its use to measure stress, including (a) the rigidity of support of the indentor and specimen, (b) the size and depth of the indentation, (c) the uniaxial stress–strain behavior of the specimen material.

Notation

C = concentration factor for stresses around an indentation
d = indentation contact diameter
D = indentor-ball diameter
n = optical-interference fringe number
$n_{\parallel}$ = fringe number along the radial line perpendicular to the load direction
$n_{\perp}$ = fringe number along the radial line perpendicular to the load direction
p = indentation depth
x = radial distance from the edge of the indentation
α = ball contact angle with original surface
σ_b = applied or residual stress in the body under consideration

Other notation is defined in the text.

John H. Underwood is associated with Materials Engineering Division, Benet Weapons Laboratory, Watervliet, NY 12189.

Paper was presented at Third SESA International Congress on Experimental Mechanics held in Los Angeles, CA on May 13-18, 1973.

Original manuscript submitted: Oct. 17, 1972. Final version received: May 7, 1973.

Introduction

During the past 40 years, several methods for measuring stress in metals have been described which are based on changes in indentation hardness measurements. Among the more recent is the work of Sines and Carlson,[1] Blain,[2] and Oppel.[3] Stress-measurement methods have also been proposed which are based on indentation tests other than the standard hardness tests. Beeuwkes[4] used the relation between indentation load and indentation depth to obtain a measure of residual stress in carbon steel. Recently, Sturm[5] described a method for measuring any combination of applied and residual stress by measuring the shape of an indentation in a metal sample. He uses the measured variation in diameter of a conical indentation to determine the direction and magnitude of stress present by considering a model of the plastic deformation caused by the indentation. Sturm's method suggested to this author a method for determining residual stress by a different type of indentation test and analysis.

We have observed, using an optical-interference method, that the permanent surface deformation around a shallow spherical indentation in alloy steel is nonsymmetrical when the indentation is made with an applied or residual stress present. The optical-interference photo in Fig. 1 shows such a nonsymmetrical deformation pattern, Fig. 1(a), around an indentation in the specimen containing tensile residual stress and a nearly symmetrical pattern, Fig. 1(b), after most of the residual stress had been relieved. As seen in the photo, the nonsymmetrical surface deformation around an indentation is a clear indication of the presence of residual stress and is easily recorded. In the following sections, the details of the method are described and various conditions are discussed which affect the use of the method as a quantitative measure of stress.

Experiments

Cylinder Test

The experimental results of Fig. 1 were obtained as follows. A 2-in.-long section of a 2-in.-OD, 1-in.-ID, 4330 steel cylinder was the test specimen. The cylinder had previously been subjected to an internal

pressure which produced circumferential strain beyond the yield strain of the material throughout the wall thickness. This procedure, termed complete overstrain autofrettage, has been shown[6] to result in a circumferential tensile residual stress at the OD of about $0.45\sigma_y$, where σ_y is the material yield stress, 158 ksi in this case.

The cylinder section was polished to produce a 0.3-in.-wide flat area on the OD (see Fig. 2). The flat area reduces the local wall thickness by a maximum of 2.2 percent and reduces the cross-section area by less than 0.1 percent; so, little effect on the residual stress in the cylinder is expected. Silicon carbide and diamond abrasives were used to produce a standard high-quality metallographic polish. The central 0.1-in. portion of the 0.3-in.-wide area was held flat within 0.00001 in. by careful control of the cylinder position during polishing.

The indentations were made with a 0.1250 ± 0.0001-in.-diam tungsten carbide ball. The ball was press fit into the end of a steel rod which was mounted in a conventional hydraulic testing machine. An indentation load of 250 lb was applied normal to the flat area, held for 5 s and released. After the first indentation was made, the cylinder wall opposite the flat was slit as indicated in Fig. 2. The second indentation was made in the same manner adjacent to the first. Thus indentation (a) in Fig. 1 was made with a tensile residual stress of 65 to 75 ksi present at the outer surface of the cylinder in the circumferential direction, vertical in the photo; indentation (b) was made with 0 to 10-ksi residual stress in the cylinder. The exact values of stress are not known due to variations in the cylinder yield behavior caused by the Bauchinger effect[6,7] and other nonidealities in the yielding of 4340 steel. This same uncertainty in the value of residual stress applies to some extent to any specimen in which the residual stress is produced by plastic deformation.

The surface displacement around the indentations in the direction normal to the surface was measured using an optical-interference technique similar to Tolansky's.[8] A glass proof plate was held in contact with the polished surface which was illuminated with thallium-vapor monochromatic light. Optical interference fringes form in the gap between the proof plate and the specimen. Each fringe corresponds to a change in displacement of the surface of about 0.00001 in. Thus, the pattern of fringes gives a detailed description of the surface-displacement gradient around an indentation. Additional information on the technique and its use to measure surface displacement can be found in Refs. 9 and 10.

The cylinder results in Fig. 1 indicate the basis of the method for measuring stress, that is, the nonsymmetrical surface deformation around an indentation made with a stress present. The next section describes a series of tests and associated analysis to determine what quantitative information can be obtained from the method.

Uniaxial Tests

Indentation tests were performed on 170-ksi yield-strength 4340 steel specimens with various values of applied uniaxial stress, both tension and compression.

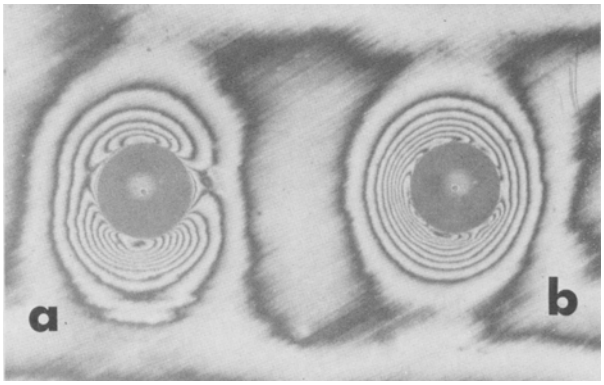

Fig. 1—Surface displacements around indentations with and without residual stress

Tests with applied tension were performed on ⅛ by ¼-in. cross-section specimens as shown in Fig. 3. The specimens were first polished in the same general manner as used with the cylinder specimens. Indentations were made in the same manner as described above using the 0.1250-in.-diam ball and 250-lb load. The tensile load was applied to the specimen before indentation and released following.* The load was applied and monitored using a hydraulic loading fix-

* *This procedure of releasing the load is not a direct simulation of residual stress which, of course, remains following indentation. However, it is the same procedure used in the results of Fig. 1, where the nonsymmetrical deformation occurred in the presence of residual stress but was photographed after the stress was relieved. Results which follow (Fig. 10) show similar nonsymmetrical deformation with the residual stress still present.*

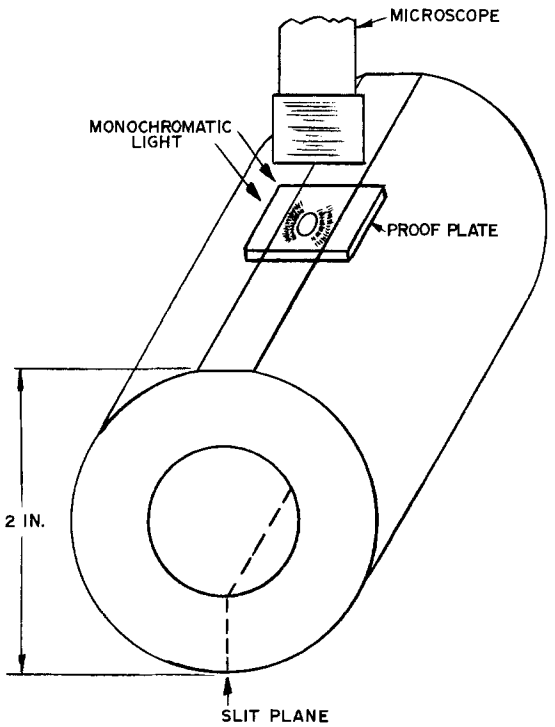

Fig. 2—Cylinder test arrangement for measuring residual stress

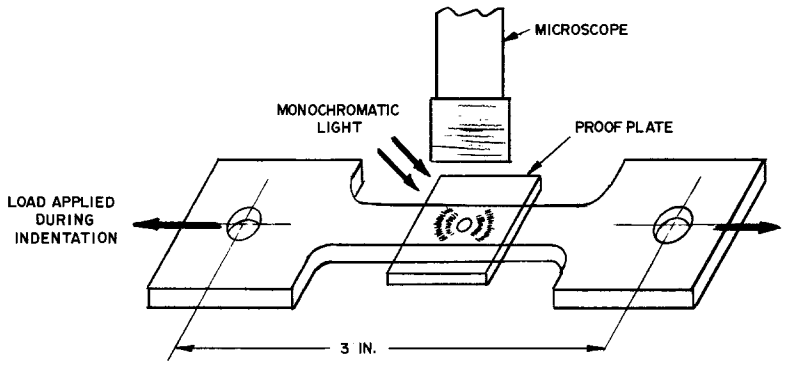

Fig. 3—Arrangement for uniaxial calibration tests

ture which includes a strain-gage load-cell pin-connected to the specimen. Indentation tests with an applied compressive stress were performed using the same loading fixture modified to apply compressive load to specimens of ⅛ by ¼-in. cross section, ½-in. long. The compressive load was measured directly with two strain gages on each specimen.

Two series of indentation tests were performed with applied tensile-stress values of 0, 30, 60 and 90 ksi. In the first series, the indentations were made with the carbide ball in a relatively short, rigid-support rod, 0.38-in. diameter by 0.50-in. unsupported length. The second series with applied tension used a longer support rod, 0.50-in. diameter by 3.0-in. unsupported length. These two methods of ball support result in different surface displacement around the indentation as will be shown and discussed in the next section. Tests with applied compressive stress of 30, 60 and 90 ksi used the short support.

Test Results and Analysis

Figure 4 shows interference photos of indentation tests using the rigid ball support with applied tensile stress, Fig. 4(a),(b),(c),(d), and with compressive stress, Fig. 4(e),(f). The original photos were taken at 20× with the load direction horizontal. The transition from a circularly symmetrical surface-deformation pattern at 0 ksi to a two-lobed pattern at 90-ksi tension is easy to see. The compression results are not as easy to interpret. They show what appears to be a shift in the pattern around the indentation, with a maximum number of interference fringes and, thus, a maximum surface displacement occurring at only one location around the indentation. The results of Fig. 5 can be used to explain this shift in the pattern. Figure 5 shows the second series of tensile indentations made with the less-rigid ball support described previously. The indentations at low stress result in the same type of fringe-pattern shift as seen in the compression tests of Fig. 4. We associate this shift in the deformation pattern with a lack of adequate support during the indentation process. The lack of support can be either (a) inadequate support of the specimen as was the case in the compression tests of Fig. 4 (due to the small specimen size) or (b)

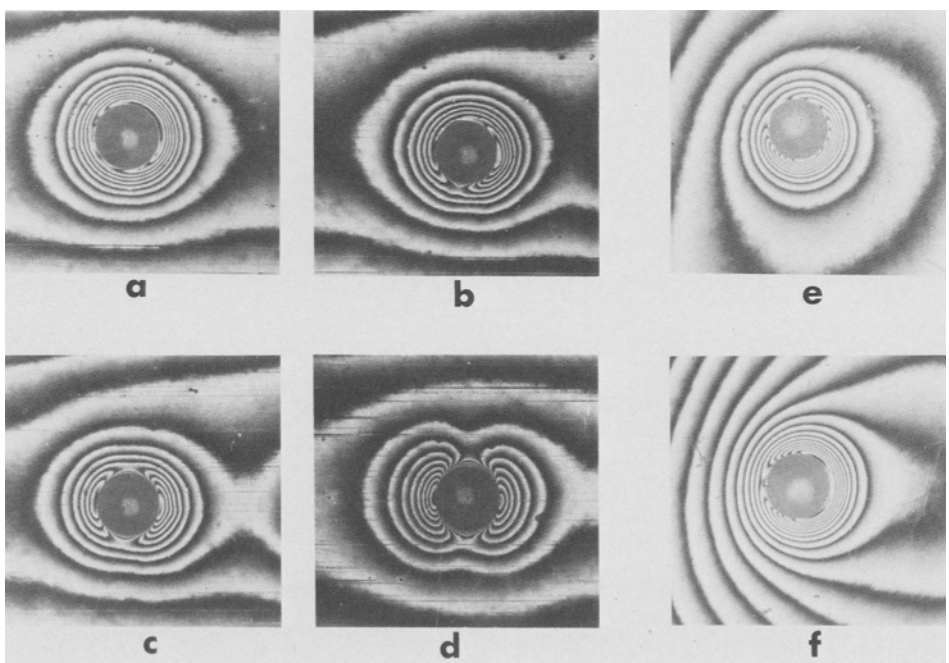

(a)-(d): 0, 30, 60, 90-ksi applied tension
(e), (f): 30, 90-ksi applied compression

Fig. 4—Interference photos of indentations with rigid support

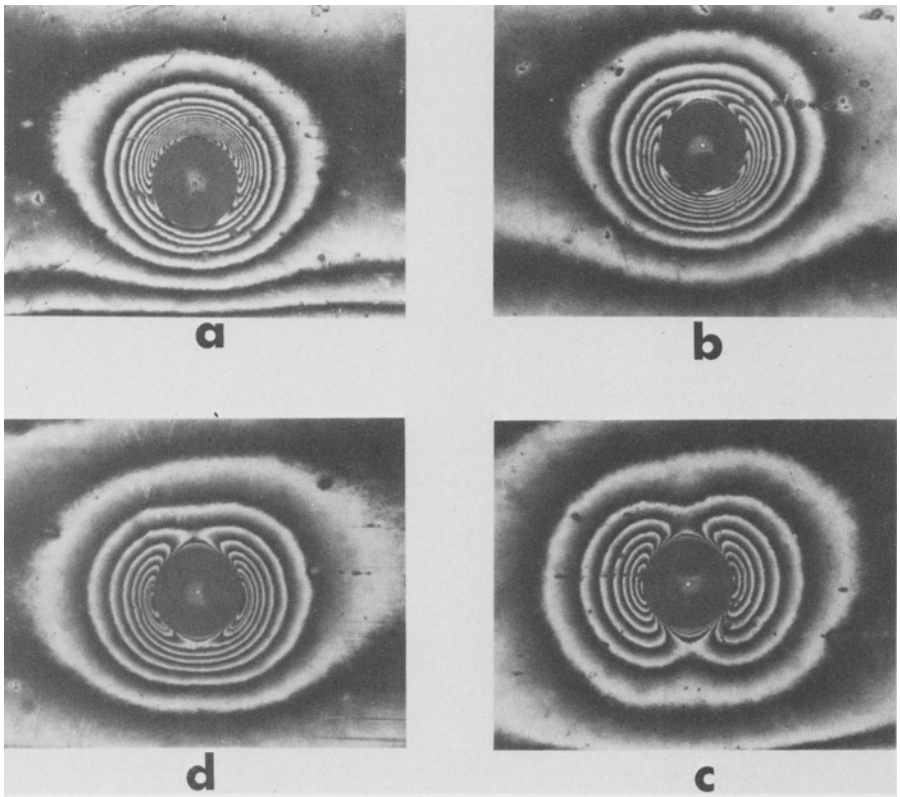

(a)-(d): 0, 30, 60, 90-ksi applied tension

Fig. 5—Interference photos of indentations with nonrigid support

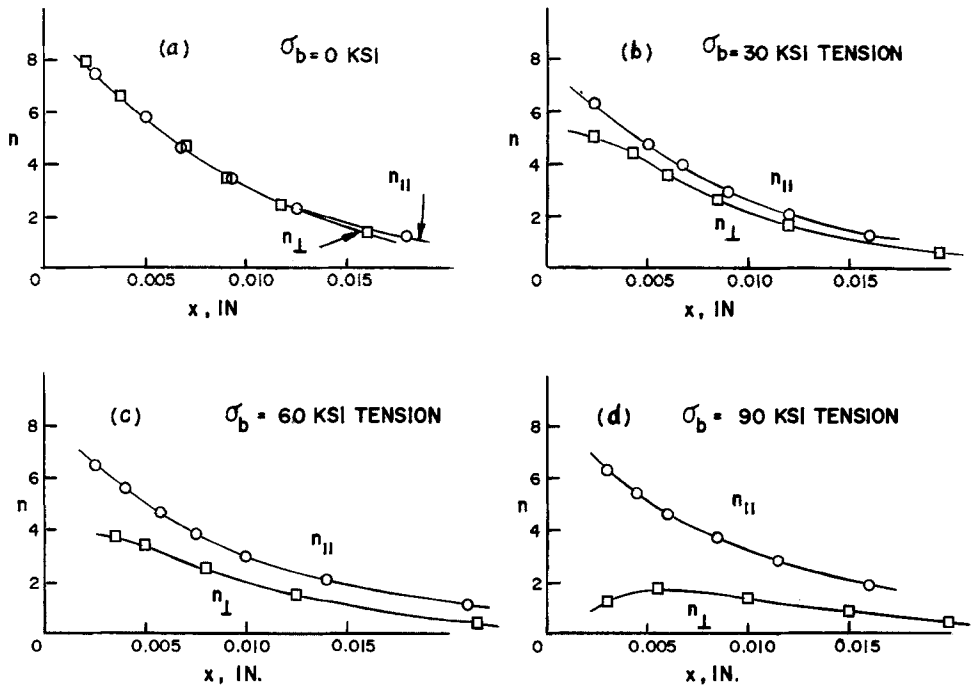

Fig. 6—Fringe-number plots from indentations with rigid support

inadequate support of the indentor ball, as was the case in the tension tests of Fig. 5 (due to the long ball support).

Results from Figs. 4 and 5 are shown in Figs. 6 and 7. The plots are simply fringe number, n, vs. the radial distance from the edge of the indentation, x. The number zero is assigned to the fringe which is judged to be closest to the indentation but still not associated with the deformation pattern. The zeroth fringe is usually located about two indentation diameters, $2d$, from the edge of the indentation. Examples of the zeroth fringe are the dark area on the far right in Fig. 4(b) and the light area on the far right in Fig. 5(b). Two sets of fringe-number data

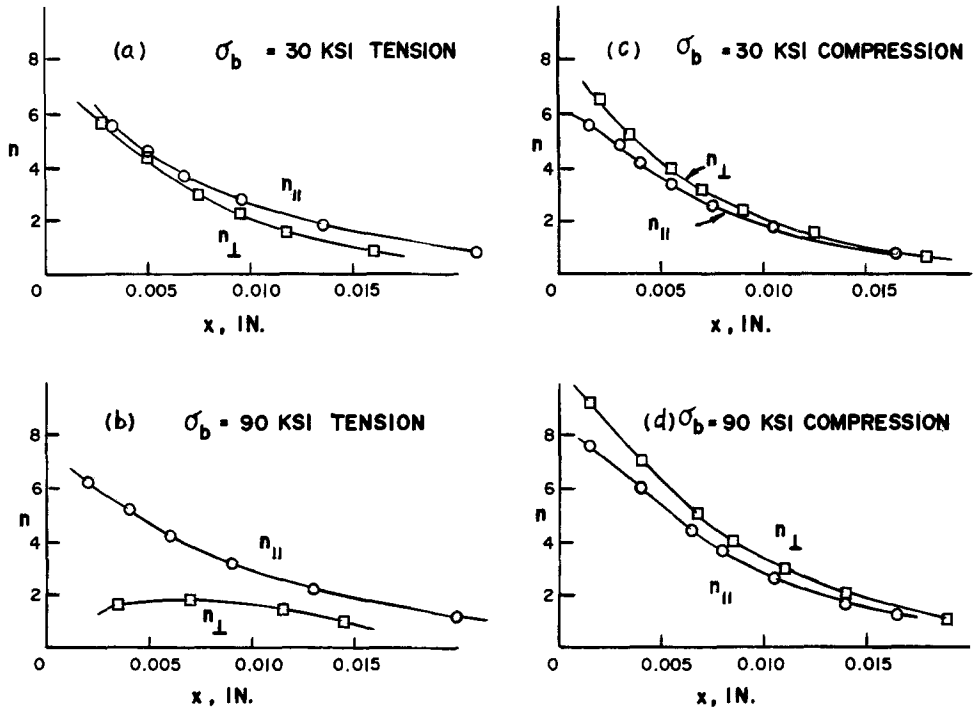

Fig. 7—Fringe-number plots from indentations with nonrigid support

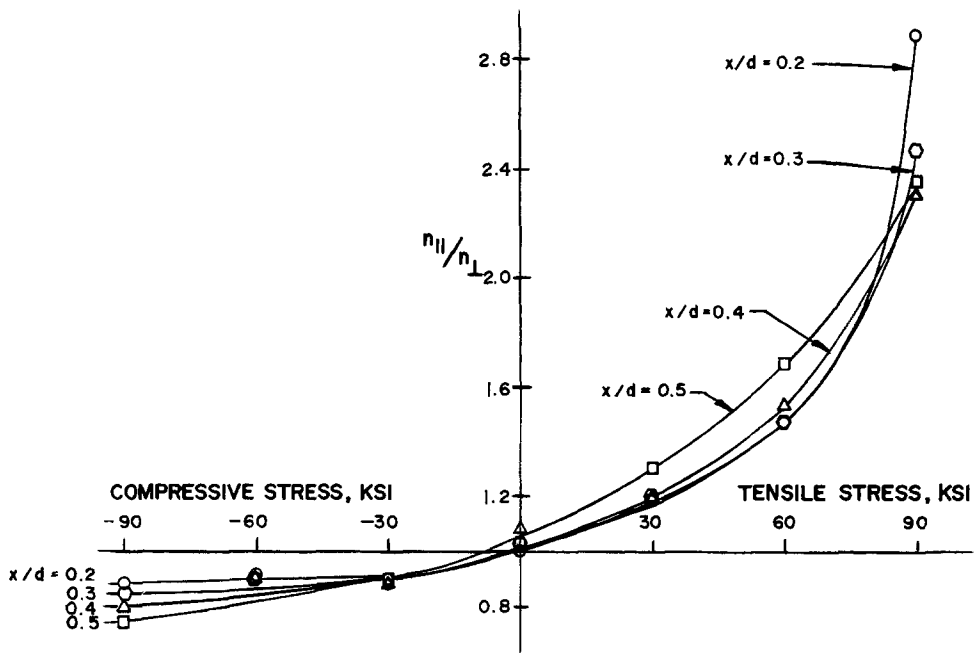

Fig. 8—Fringe-ratio calibration plot for 4340 steel

are shown on each plot, the data taken along the radial line parallel to the load direction, denoted $n_{||}$, and the data along the radial line perpendicular to the load, $n_{\perp}$. Each data point is, in reality, the average of the two n values measured on opposite sides of the indentation at the same distance from the edge.

Three aspects of the data in Figs. 6 and 7 should be noted. (1) The average fringe number along the line perpendicular to the load direction, $n_{\perp}$, decreases relative to the average fringe number parallel to the load direction, $n_{||}$, as the applied tensile stress increases. (2) This decrease in $n_{\perp}$ relative to $n_{||}$ is not greatly affected by the use of the less-rigid, long ball support during indentation [Figs. 7(a) and 7(b)] and by the accompanying shift in the fringe pattern. (3) For compressive loads, the average fringe number along the line parallel to the load direction, $n_{||}$, decreases relative to $n_{\perp}$ with increasing stress [Figs. 7(c) and 7(d)]. This effect is opposite that observed for tensile loads.

A summary of the indentation test results is shown in Fig. 8. The ratio of the average fringe number along the line parallel to the load to the average fringe number along the line perpendicular to the load, $n_{||}/n_{\perp}$, is plotted vs. the value of the applied stress. The values of fringe ratio were calculated from Figs. 6 and 7 and similar plots at the values of x/d shown.

Smaller or larger x/d values are not recommended for this material and test procedure; the fringe-position measurement becomes less accurate for small values of x, and the fringe positions become more affected by the nonflatness of the original surface for large x. An x/d of 0.3 appears to be the best compromise for these data.

It is clear from Fig. 8 that there is a much larger change in fringe ratio with tensile stress than with compressive stress. Thus, for this material and condition, the indentation method can be used to measure tensile residual stress with an estimated error of 10 ksi or less, whereas the method can confidently be used only to detect the presence of compressive stress. The general procedure for measuring tensile residual stress would be (a) polish and indent the surface of the 4340 steel sample to be tested; (b) take an interference photo of the indentation and calculate the fringe ratio at $x/d = 0.3$; (c) obtain the residual-stress value from the uniaxial calibration curve in Fig. 8.

Indentation Model

A qualitative model of the indentation process and a discussion of selected variables which affect the process are offered here.

Consider an indentation in a body with an applied or residual stress present, as sketched in Fig. 9. The circularly symmetrical surface-deformation pattern observed with no stress present [Fig. 4(a)] is the expected "crater lip" effect caused by an indentation, shown exaggerated in the sketch. The two-lobed deformation pattern which occurs with a body stress present could be accounted for by the interaction of the body stress with the indentation stress during the plastic deformation caused by the indenta-

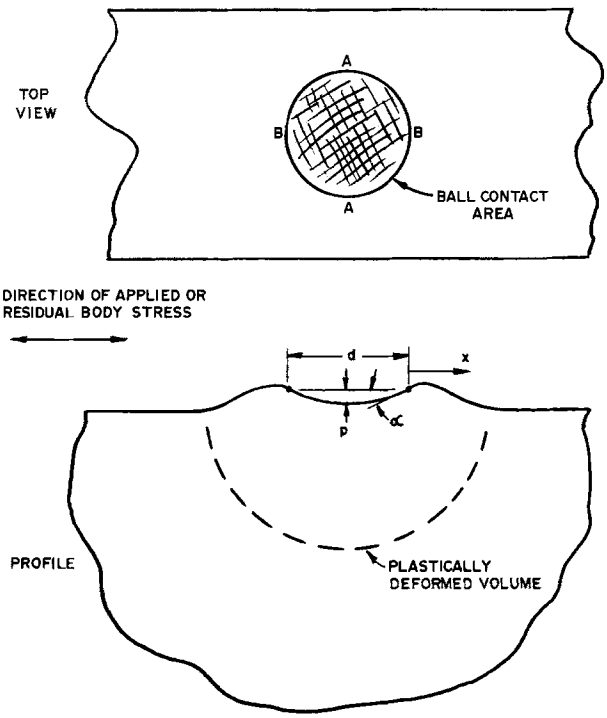

Fig. 9—Schematic of indentation geometry

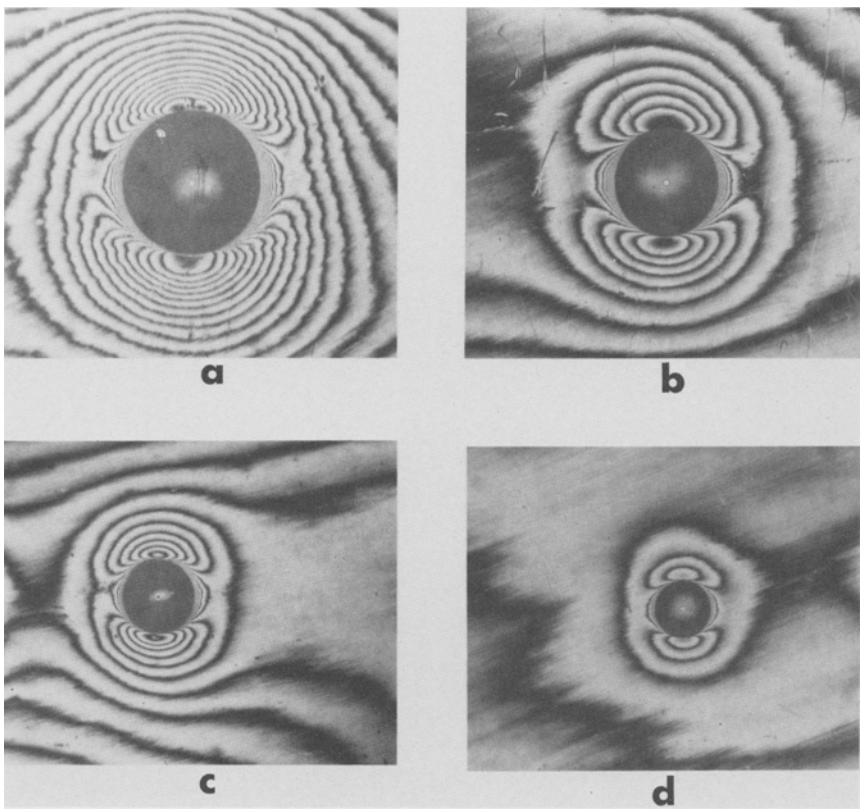

(a), (b): D = 0.2500 in.; indentation load = 1000 lb, 500 lb
(c), (d): D = 0.1250 in.; indentation load = 250 lb, 125 lb

Fig. 10—Interference photos of various-size indentations

tion, then so would the plastic deformation and the resulting surface displacement. Increases and decreases in the body stress can be envisioned by considering that the overall plastic deformation beneath the indentation acts somewhat like a hole. The plastically deformed volume supports stress only up to the material yield stress, so that one could expect some concentration of stress around the edge of the deformed volume. The stress concentration would not be of the same magnitude as around a hole which can support no stress within, but there could be enough concentration of stress to affect the yielding and surface displacement around the indentation.

Using the Tresca yield condition and the above reasoning, the observed differences in surface displacements in the directions perpendicular and parallel to the load direction can be explained. Tresca yielding is controlled by the maximum principal-stress difference. The largest principal stress during indentation is assumed to be the compressive stress beneath the indentor in the direction normal to the surface. With a tensile body stress present, any concentration of the tensile stress at points A (see Fig. 9) will further aid the compressive yielding during indentation and will result in less upward surface displacement after indentation, as was observed. An expression for the principal-stress difference at points A, with a compressive indentation stress of magnitude σ_i and a tensile body stress of magnitude σ_b is:

$$\sigma_1 - \sigma_3 = (-\sigma_i) - (+\sigma_{b\cdot C}) \qquad (1)$$

If the concentration factor, C, is greater than $+1.0$ (but not necessarily approaching $+3.0$, the value for a hole in an elastic plate) a noticeable effect on the yielding and surface displacement would be expected at points A.

With a compressive body stress present, the maximum principle-stress difference would occur at points B:

$$\sigma_1 - \sigma_3 = (-\sigma_i) - (-\sigma_{b\cdot C}) \qquad (2)$$

Any concentration factor below 0 (but not necessarily approaching -1.0, the value for a plate) would result in favored compressive yielding and less upward surface displacement at points B relative to A, as was observed. It should be noted that eqs (1) and (2) are intended to describe the dominant stresses in general locations just outside and beneath the edge of the indentation. The equations are not intended to calculate exact stress values at specific points.

A final comment regarding the model is that it includes a larger potential effect on the surface deformation with a tensile body stress than with a compressive stress because of the larger stress-concentration factor in the analogous tension-plate solution. A larger effect on surface deformation was observed with a tensile stress as discussed earlier in reference to Fig. 8.

The effects of ball diameter, D, and indentation depth, p, on the indentation process are worth considering. Figures 10(a) and 10(b) are interference photos of indentations made with a 0.2500-in. carbide ball at 1000-lb and 500-lb loads; Figs. 10(c) and 10(d) are with the 0.1250-in. ball described previously at 250-lb and 125-lb loads. The specimen is a section of the same 2-in.-OD cylinder described previously. The tensile residual-stress direction is vertical as before. The two-lobed deformation pattern is qualitatively similar for all indentations. This similarity can also be seen in a normalized plot of the indentation results, see Fig. 11. The distance from the edge of the indentation, x, is normalized by the indentation diameter, d. The fringe number, n, a direct measure of the upward surface displacement, is normalized by the downward displacement of the indentor, i.e., the indentation depth, p. The values of p are calculated from the geometric interrelation with ball diameter, D, contact diameter, d, and contact angle, α:

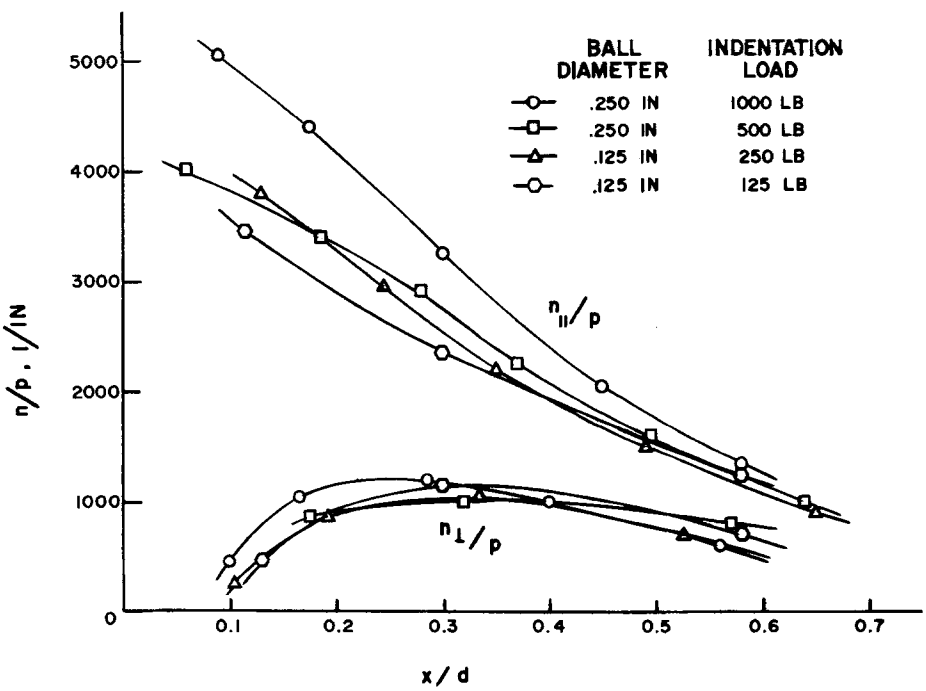

Fig. 11—Normalized fringe-number plots from various-sized indentations

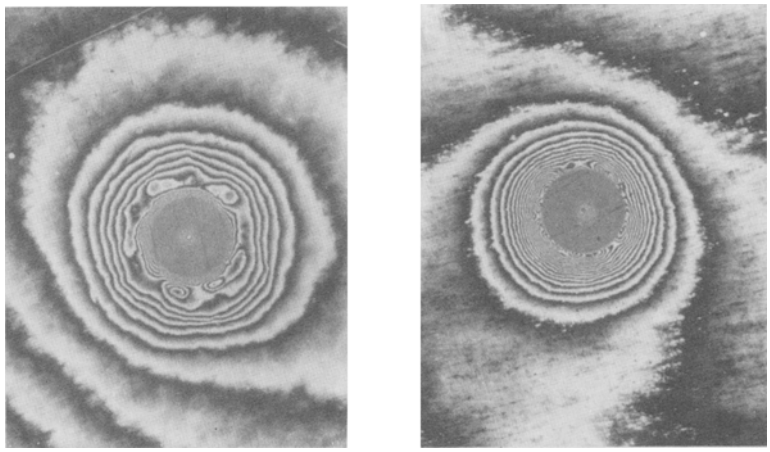

a b

(a): 1018 steel
(b): 6061-T6 aluminum

Fig. 12—Interference photos of indentations in mild steel and aluminum

$$\sin \alpha = d/D$$

$$p = (1 - \cos \alpha) D/2 \qquad (3)$$

The largest deviation in Fig. 11 corresponds to the largest indentation for which the assignment of the zeroth fringe is least certain. This is due to the large fringe pattern in Fig. 10(a) extending beyond the central flat area on the cylinder.

Two further comments regarding the indentation process in relation to the above discussion are as follows: (1) The average contact diameter observed in Figs. 4 and 5 is $d = 0.026$ in. The corresponding indentation depth calculated from eq (3) is $p = 0.0014$ in. This value applies only while the indentation load is applied. The indentation depth after the indentation load is removed is somewhat less due to reverse upward yielding of the material under the indentor. (2) The selection of $x/d = 0.3$ as the best value for calculating the fringe ratio is supported by the results of Fig. 11. At $x/d = 0.3$, $n_{\parallel}$ and $n_{\perp}$ are large enough to be measured with good relative accuracy while, at the same time, not in the range where the n values change rapidly with x.

Finally, some idea of the effect of specimen-material properties on the indentation process can be seen in Fig. 12. The indentations shown are in 1018 steel annealed at 1600° F, Fig. 12(a), and 6061-T6 aluminum, Fig. 12(b), both with no stress present. The irregular fringes around the indentation in 1018 steel are caused by the yield point instability and Luder's strain characteristic of this material.[10] This irregular deformation may affect the accuracy of stress measurements by indentation, but the same type of results as obtained with alloy steel should be possible. The high concentration of fringes near the edge of the indentation in the 6061 aluminum is caused by the relatively low strain hardening in this alloy which has a strain-hardening exponent of 0.04.[10] The best indentation results with this alloy and others with low strain hardening would be obtained with shallow indentations, that is, with a small p/d ratio. A small p/d should result in less concentrated deformation near the edge of the indentation and, thus, less concentrated fringes which are easier to interpret.

In summary, the significant aspects of this method of measuring residual stress are the following. (1) The method is essentially nondestructive, since the indentation is made by a shallow penetration of a smooth ball. (2) The experimental data, i.e., the displacements around the indentation which are used to determine stress values, are graphic and are easily measured and recorded. (3) The experimental data can be qualitatively predicted by a simple model involving the Tresca yield condition and the elastic stresses around a hole. (4) The experimental technique is inherently sensitive, since the unit of measurement in optical interference is the wavelength of a visible light. (5) The method can be used to measure uniaxial tensile residual stress; for uniaxial compression and for biaxial tension with near equal values of stress, the method is by nature less sensitive and is affected by shifts in the deformation pattern due to inadequate support during indentation.

Acknowledgment

The author compliments Charles DeLaMater for his handling of the experimental phases of this work. Also, he thanks James Vergow and David Kendall for their help and advice during the work.

References

1. Sines, G. and Carlson, R., "Hardness Measurements for Determination of Residual Stress," ASTM Bulletin 35-37 (Feb. 1952).

2. Blain, P. A., "Influence of Residual Stress on Hardness," Metal Progress, 71, 99-100 (Jan. 1957).

3. Oppel, G. U., "Biaxial Elasto-plastic Analysis of Load and Residual Stress," EXPERIMENTAL MECHANICS, 4 (5), 135-140 (1964).

4. Beeuwkes, A., "Plastic Flow and Fracturing of Metals," Watertown Arsenal Lab. Tech. Report #53–893/154–11, ed. by G. Sachs (Apr. 1954).

5. Sturm, R. G., "The Total Stress Gage," Tech. Note 001, Sturm–Stress, Inc. (Nov. 1970); also presented at 1968 SESA Spring Meeting held in Albany, N. Y. (May 7-10).

6. Kendall, D. P., "The Effect of Material Removal on the Strength of Autofrettaged Cylinders," Watervliet Arsenal Tech. Report WVT-7003 (Jan. 1970).

7. Milligan, R. V., Koo, W. H. and Davidson, T. E., "The Bauschinger Effect in a High Strength Steel," Trans. ASME, J. of Basic Eng., 88, 480-488 (June 1966).

8. Tolansky, S., "Multiple-Beam Interferometry in Analytical Metallography," Metallography, 2, 1-18 (1969).

9. Underwood, J. H. and Kendall, D. P., "Measurement of Microscopic Plastic-strain Distributions in the Region of a Crack Tip," EXPERIMENTAL MECHANICS, 9 (7), 296-304 (1969).

10. Underwood, J. H., Swedlow, J. L. and Kendall, D. P., "Experimental and Analytical Strains in an Edge-Cracked Sheet," Engn. Fracture Mech., 2, 183-196 (1971).